ASTRONOMY & ASTROPHYSICS
SUPPLEMENT SERIES

Astron. Astrophys. Suppl. Ser. **114**, 549-556 (1995)

Stellar models for a wide range of initial chemical compositions until helium burning. II. From X=0.63 to X=0.80, for Z=0.01*

A. Claret[1,**] and A. Giménez[2]

[1] Instituto de Astrofísica de Canarias, E-38200 La Laguna, Tenerife, Spain
[2] Laboratorio de Astrofísica Espacial y Física Fundamental, INTA, Apartado 50727, E-28080 Madrid, Spain

Received May 4; accepted June 22, 1995

Abstract. — Three new grids of stellar evolutionary models with Z=0.01 are presented for the following values of initial hydrogen content $X_{\rm i}$ = 0.80, 0.73 and 0.63. The latest set of radiative opacities with spin-orbit coupling provided by the Lawrence Livermore group are used. For the lower temperatures the results by Alexander were considered. The models were computed taking into account core overshooting and mass loss. The grids cover the mass range between 1 and 40 $M_{\odot}$. The internal structure constants (k_j, j = 2, 3, 4) and the moment of inertia are also computed. These parameters are needed to investigate apsidal motions and tidal interactions in double-lined eclipsing binaries. This paper is part of a project which aims to provide grids of stellar models for a wide range of metal and hydrogen content.

Key words: binaries: general — stars: evolution; interiors; fundamental parameters; abundances

1. Introduction

As commented in the previous paper of the present series (Claret 1995, hereafter Paper I) there are several sets of stellar models available in the astrophysical literature, but they are very limited in the helium content range for a given metallicity. The helium content is often assumed to be that derived from available enrichment laws though this value may not represent the "best" one given the uncertainties involved in the process. In fact, errors in the primordial helium determination, uncertainties in the enrichment laws and error bars in the metallic content, indicated us the need to have grids of models, centered in some selected metallicities, but with several helium content values bracketing those predicted by the assumed enrichment law.

With this purpose in mind, we computed three grids of models centered in the solar metallicity in Paper I. The interval in the hydrogen content was taken to be 0.10. For the present paper we adopted Z=0.01 and also selected three compositions around X=0.73. Of course the chemical composition (X, Z)=(0.80, 0.01) is not compatible with a primordial helium value equal to 0.24 since this would mean a negative derivative $\Delta Y/\Delta Z$. The same holds for (X, Z)=(0.80, 0.02) in Paper I. These extreme values of initial hydrogen content were selected only to permit interpolations in chemical compositions given the uncertainties in the chemical composition and in the primordial helium abundance. We present essentially the results of the model computations without getting into a detailed explanation of the physical implications of such calculations.

The main characteristics of the input physics used in the present models can be summarized as follows:

1. Mass loss rate during the main sequence was computed through the formula by Nieuwenhuijzen & de Jager 1990.
2. For the red giant phase, we have adopted the results by Reimers 1977.
3. Convection was treated using the mixing length theory and the adopted mixing length parameter was $l/H_{\rm p}$ = 1.52 where $H_{\rm p}$ is the the so-called scale height of pressure and is given by $-{\rm d}r/{\rm dln}P$.
4. For models with convective cores, we considered a moderate overshooting characterized by $\alpha_{\rm ov}$ = d$/H_{\rm p}$ = 0.20. For less massive stars the size of the convective cores are often smaller or of the same order of one scale

*Tables 1-72 are available in electronic form at the CDS: see the Editorial in A&AS 1994, Vol. 103, No. 1

**Present address*: Instituto de Astrofísica de Andalucia, Apartado 3004; 18080 Granada, Spain
e-mail: claret@iaa.es

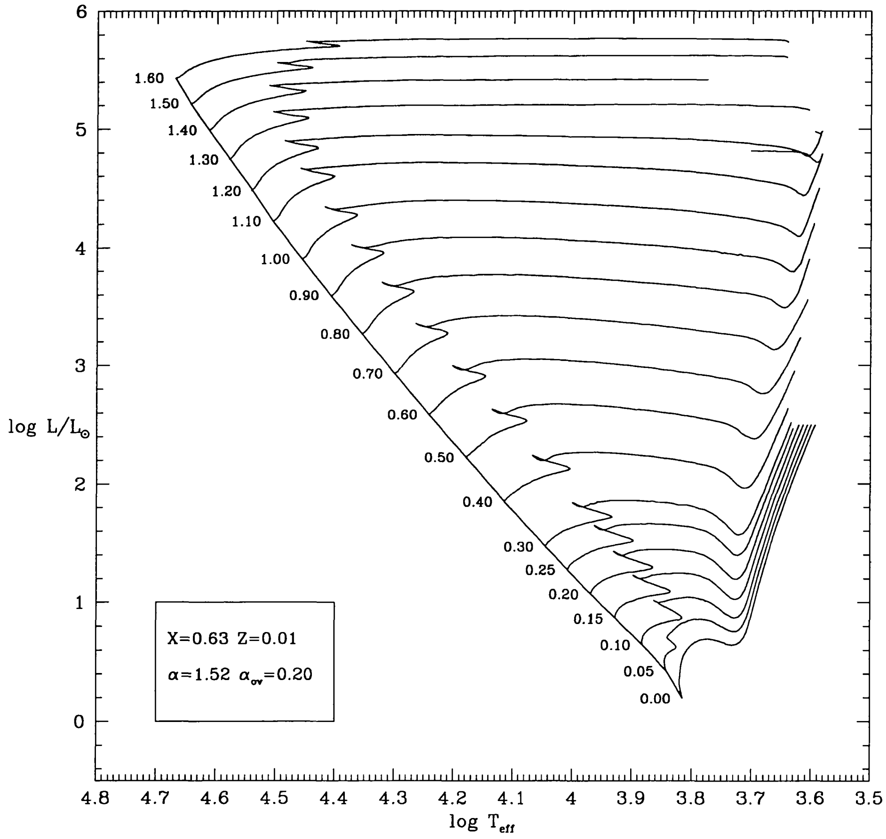

Fig. 1. HR diagram for the grid X63. Numbers attached denote log M

height of pressure at the border of the core. In these cases we have used a simple algorithm $\alpha_{\rm ov}$ = min (0.20 d/$H_{\rm p}$, 0.20 $R_{\rm c}$) where $R_{\rm c}$ is the size of the core given by the Schwarzschild criterion for convection. For this complicated mass range we can provide under request models computed using the classsical criterion for convection and/or with a smaller $\alpha_{\rm ov}$.

5. The new radiative opacities with spin-orbit coupling computed with OPAL code (Iglesias et al. 1992) were used throughout except for temperatures lower than 6000 K and greater than 1–5 10^8 K. In these cases, we have used the tables provided by Alexander (1992) and the computations from Los Alamos (Huebner et al. 1977), respectively.
6. The nuclear network considers the CNO cycle and the three pp-chains and for the helium burning we adopted the reactions,
^{4}He$(\alpha,\gamma)^8$Be$(\alpha,\gamma)^{12}$C(α,γ) ^{16}O$(\alpha,\gamma)^{20}$Ne.
However, since our interest is main sequence stars (mainly double-lined eclipsing binaries), we have stopped the calculations in the first stages of helium burning. During this stage, as the nuclear reactions ^{14}N$(\alpha,\gamma)^{18}$F$(e^+,\nu)^{18}$O(α,γ) ^{22}Ne do not contribute significantly to energy generation, they were not considered unless a more detailed treatment of the nucleosynthesis is required. The nuclear rates were taken from Fowler et al. 1975; Harris et al. 1983; Caughlan et al. 1985 and Caughlan & Fowler 1988 and the screening factors from Graboske et al. 1973. The neutrino loss rates are from Munakata et al. 1985.
7. The equation of state takes into account partial ionization through Saha's approximation, the pressure of gas and radiation as well as the equations for degenerate electrons. Optionally, models can be computed using the MHD equation (Hummer & Mihalas 1988; Däppen et al. 1988; Mihalas et al. 1988) or CEFF (Christensen-Dalsgaard 1991; Christensen-Dalsgaard & Däppen 1992) which is a modified version of the equation of state by Eggleton et al. 1973 incorporating the coulombian-pressure correction.

Some comments on the theoretical apsidal motion constants and their applicability as well as a description of the evolutionary tracks are given in the following section.

2. The evolutionary tracks

The distortion of the stellar configurations in eccentric binary systems due to tides and rotation changes secularly the position of the periastron. The rate at which this position changes with time depends, among another parameters, on the internal structure of the stars (see e.g. Kopal 1978) through some parameters known as internal

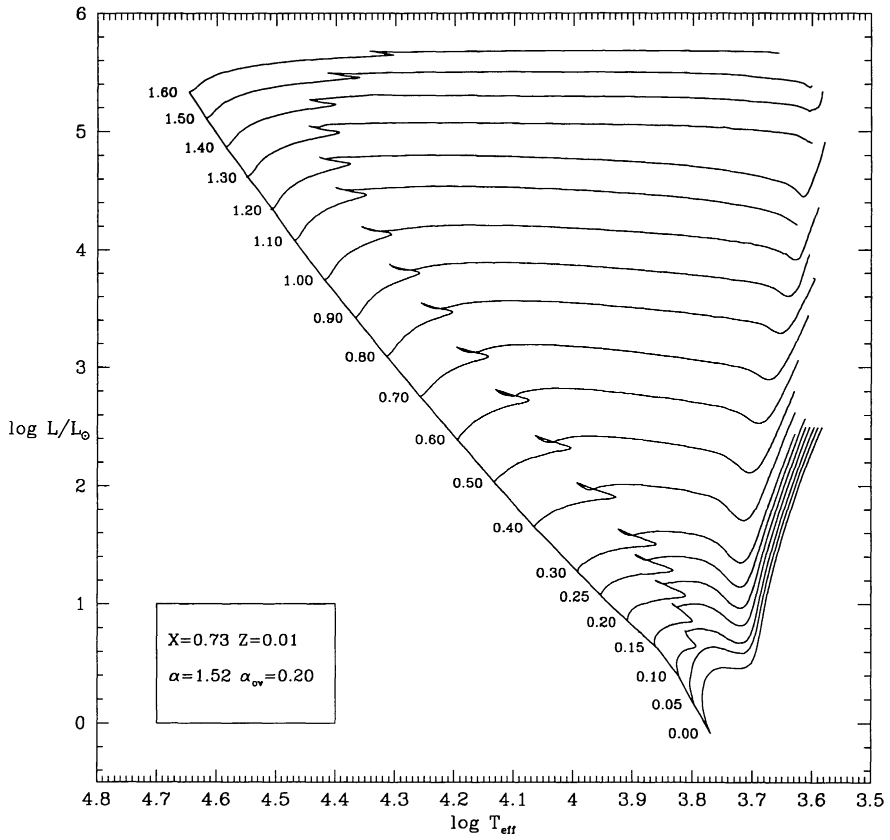

Fig. 2. HR diagram for the grid X73. Numbers attached denote log M

structure constants, log k_j (for j = 2, 3, 4). In order to make available these internal structure constants for the whole grid of computed models, we have used the Runge-Kutta method of fourth order to integrate the Radau equation for j=2, 3, 4. The corresponding values of the deviation of the equipotential surfaces from spherical symmetry provides us (in the surface of the model) with the values of k_j. For more details about apsidal motion and the comparison of theoretical predictions with observational data we refer to the works by Claret & Giménez 1993, Paper I, and references given therein.

On the other hand, synchronization and circularization times in close binary systems depend on the radius of gyration (in some theories, they depend on the apsidal motion constant k_2 (see Zahn 1977)). In order to extend the applicability of the present models to this kind of investigation, we have also computed the radius of gyration β using a similar numerical method as for the k_j.

The usual HR diagrams for the chemical compositions (X, Z)= (0.63, 0.01), (0.73, 0.01) and (0.80, 0.01), for simplicity named, X63, X73 and X80, respectively, are shown in Figs. 1-3. The expected effects in the effective temperature, luminosity and radius of changing the hydrogen content for a given metallicity can be easily checked as pointed out in Paper I. The discussion presented there about the dependence of the effective temperatures and radii on the mean molecular weight can be also applied in the present case and we do not repeat the same arguments here. Diagrams showing the effective temperatures and the surface gravities, which are useful for studies of binary with good absolute dimensions, are shown in Figs. 4-6.

At this point it is interesting to explore what are the differences between the present models and those described in the Paper I. Essentially, the basic difference is the metal content (Z=0.02 and 0.01) though a little difference is also present in the hydrogen content (ΔX=0.03). Some selected models are shown in Fig. 7. We have selected only some few models for the sake of clarity. Due to the lighter metal content, the present models are hotter and more luminous than those with Z=0.02 for a given mass (opacity effect) as expected.

On the other hand, the value of the mass for which it first appears a significant convective core is very dependent on the hydrogen content for a given metallicity. Rich mixtures in hydrogen imply that the model for which a convective core is developed should be more massive. This can be noticed by inspecting Figs. 1-3 or more explicitely through Fig. 8.

The stellar radii on the ZAMS are not significantly affected by the adopted hydrogen content, for a fixed metallicity, in the range of initial masses above 2.2 $M_\odot$. In fact,

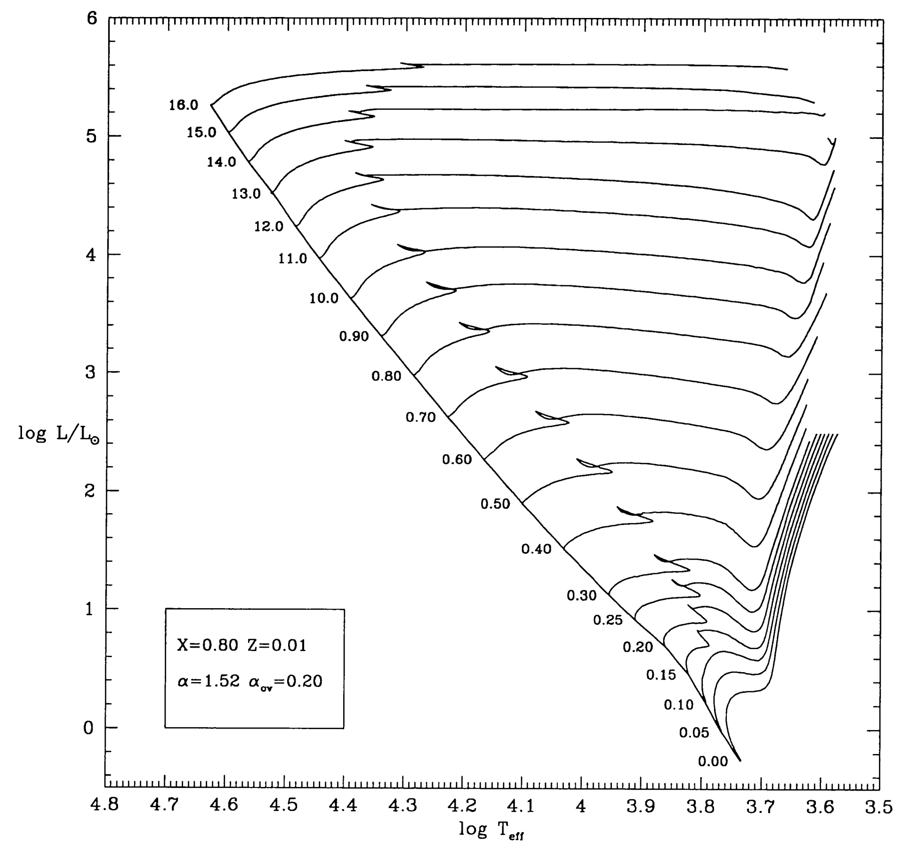

Fig. 3. HR diagram for the grid X80. Numbers attached denote log M

Fig. 9 shows this almost homologous behaviour. The average slope is equal to ≈ 0.56. However, for less massive models, the situation is different (see right bottom of Fig. 9). For the interval $0.0 \leq \log M/M_\odot \leq 0.07$ the slope is the same for the three cases but in general larger than 0.56. This deviation of such an homologous behaviour is due to the decreasing of the effective temperatures which lead to deeper outer convective zones. The net effect is to decrease the stellar radius.

Finally, the internal structure constants derived from the present models (represented by log k_2) are shown in Fig. 10. Mass concentration is directly connected with hydrogen content for models more massive than about 1.7 $M_\odot$. The differences in log k_2 are around 0.03. For models with smaller masses, the situation is inverted since hydrogen poor models are more concentrated in mass towards the center and the differences are larger, and highly mass dependent. This change of behaviour is a consequence of the change of the main source for hydrogen burning from the CNO cycle to the pp-chain.

The three grids are presented in form of 72 tables which can be obtained through the CDS or electronic mail. These tables contain the basic parameters like luminosity, surface gravity, effective temperature, apsidal motion constants, and moment of inertia, as a function of age. The stellar mass at a given time can be obtained from the surface gravity and the stellar radius, where this is defined by effective temperature and luminosity. The initial mass is given in a separate file "Readme". Tables 1 up to 24 refer to models with $X_{\rm i}$=0.63 and tables 25 up to 48 concern models with $X_{\rm i}$=0.73. Models with $X_{\rm i}$=0.80 are presented in Tables 49-72.

In several cases of stellar evolution research, models with precise mass and/or chemical composition are needed. For example, in eclipsing binary systems the masses and radii can be obtained with high accuracy. In order to compare these data with theoretical predictions, one requires stellar models computed for the observed masses and, if possible, observed chemical composition. These procedure would avoid interpolations in the grids. Such calculations as well as isochrones are available upon request (email: claret@iaa.es or aclaret@iac.es) including models in the Pre Main-Sequence phase.

Acknowledgements. We would like to thank Dr. G. Meynet for useful suggestions. The Spanish DGYCIT (PB91-0530, PB91-0526) and CICYT (PB92-0731) are gratefully acknowledged for support during the development of this work.

References

Alexander D.R., 1992 (private communication)

Caughlan G.R., Fowler W.A., Harris M.J., Zimmermann B.A., 1985, Atomic Data Nucl. Data Tables 32, 197

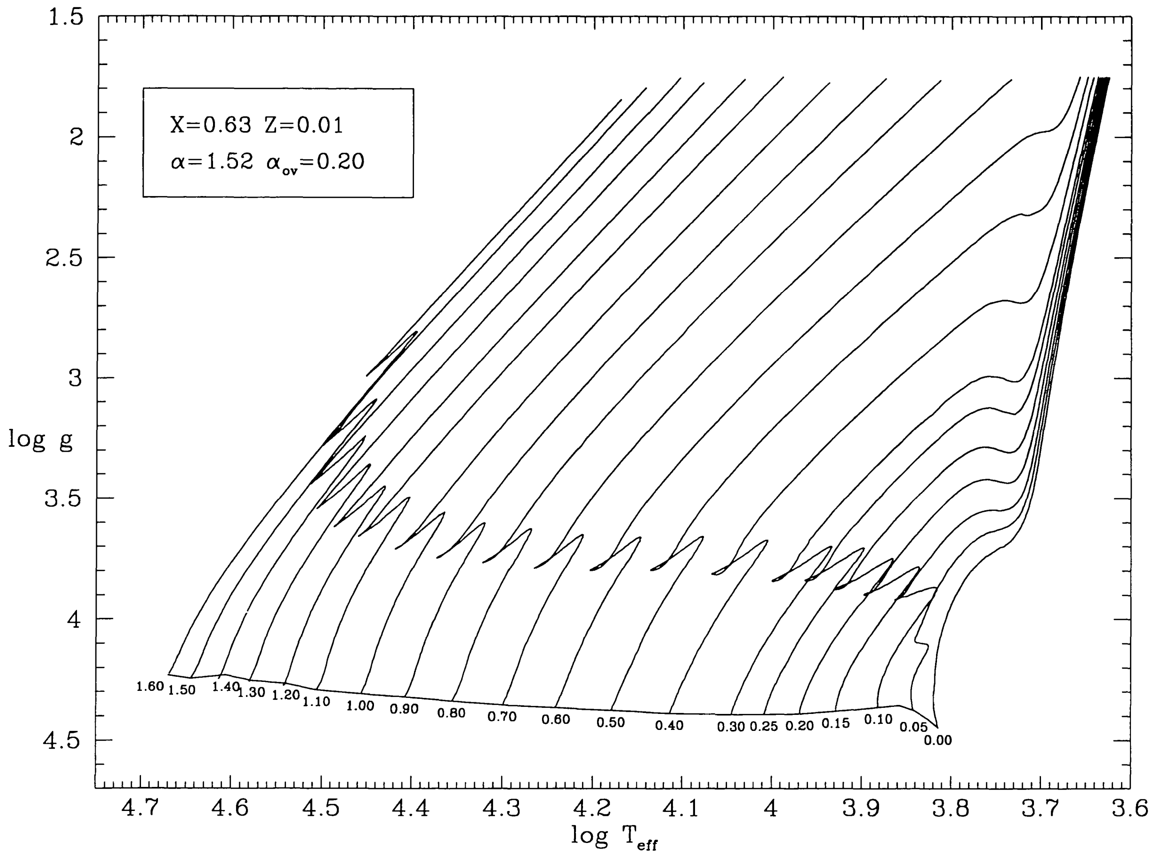

Fig. 4. Log g –log $T_{\rm eff}$ diagram for the grid X63. Numbers attached denote log M

Caughlan G.R., Fowler W.A., 1988, Atomic Data Nucl. Data Tables 40, 283

Claret A., 1995, A&AS 109, 441 (Paper I)

Claret A., Giménez A., 1993, A&A 277, 487

Christensen-Dalsgaard J., 1991, in Challenges to Theories of the Structure of Moderate-Mass Stars. In: Gough D., Toomre J. (eds.) (Lectures Notes in Physics, Vol. 388). Spring-Verlag, p. 11

Christensen-Dalsgaard J., Däppen W., 1992, A&AR 4, 267

Däppen W., Mihalas D., Hummer D.G., Mihalas B.W., 1988, ApJ 332, 261

Däppen W., 1993, in Inside the Stars, (IAU Symp. 137). In: Weiss W.W., Baglin A. (eds.) PASPC, 208

Eggelton P.P., Faulkner J., Flannery G.P., 1973, A&A 23, 261

Fowler W.A., Caughlan G.R., Zimmermann B.A., 1975, AR&A 13, 69

Graboske H.C, de Witt H.E., Grossman S.S., Cooper M.S., 1973, AJ 181, 457

Harris M.J., Fowler W.A., Caughlan G.R., Zimmermann B.A., 1983 AR&A 21, 165

Huebner W.F., Merts A.L., Magge N.H., Argo M.F., 1977, Los Alamos Scientific Laboratory Report, LA-6760-M

Hummer D.G., Mihalas D., 1988, ApJ 331, 794

Iglesias C.A., Rogers F.J., Wilson B.G., 1992, ApJ 397, 771

Kopal Z., 1978, Dynamics of Close Binary Systems. D. Reidel, Dordrecht, Holland

Mihalas D., Däppen W., Hummer D.G., 1988, ApJ 331, 815

Munakata H., Kohyama Y., Itoh N., 1985, ApJ 296, 197

Nieuwenhuijzen H., de Jager C., 1990 A&A 231, 134

Reimers D., 1977, A&A 61, 217

Zahn J.P., 1977, A&A 57, 383

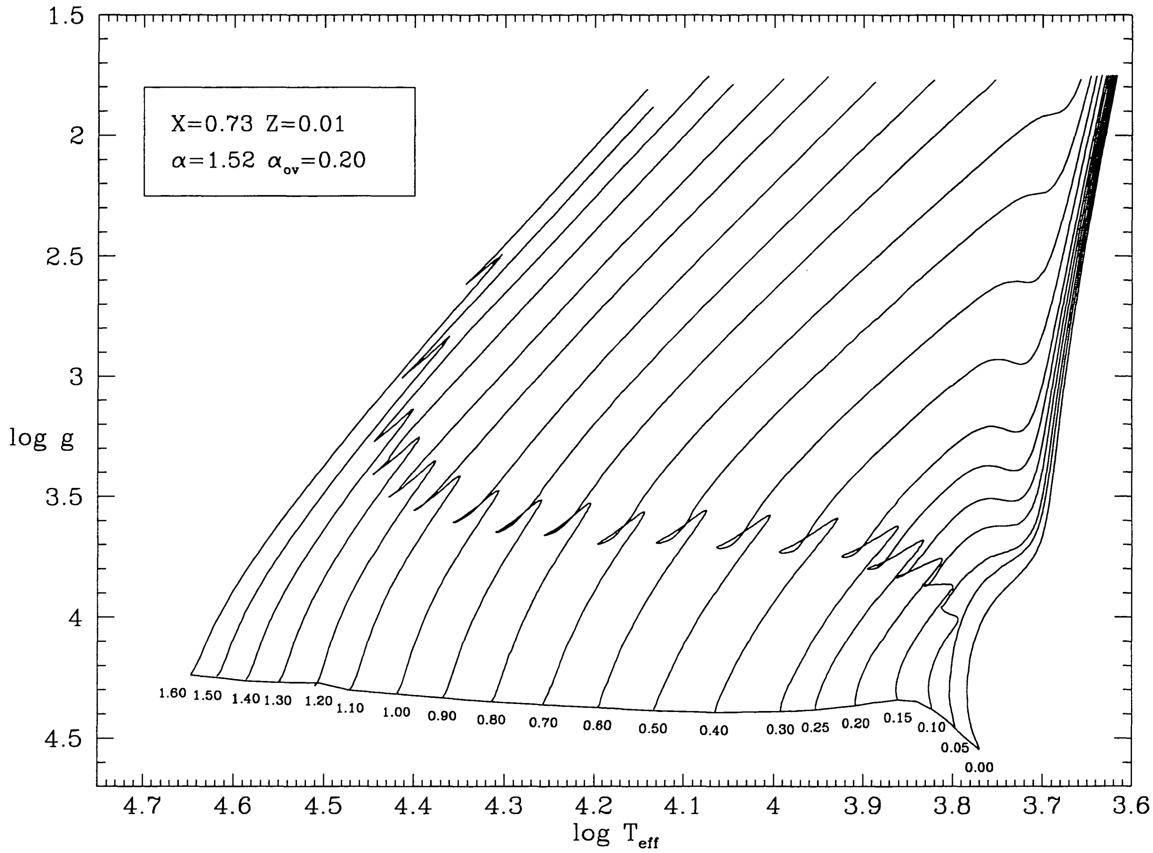

Fig. 5. Log g $-$log $T_{\rm eff}$ diagram for the grid X73. Numbers attached denote log M

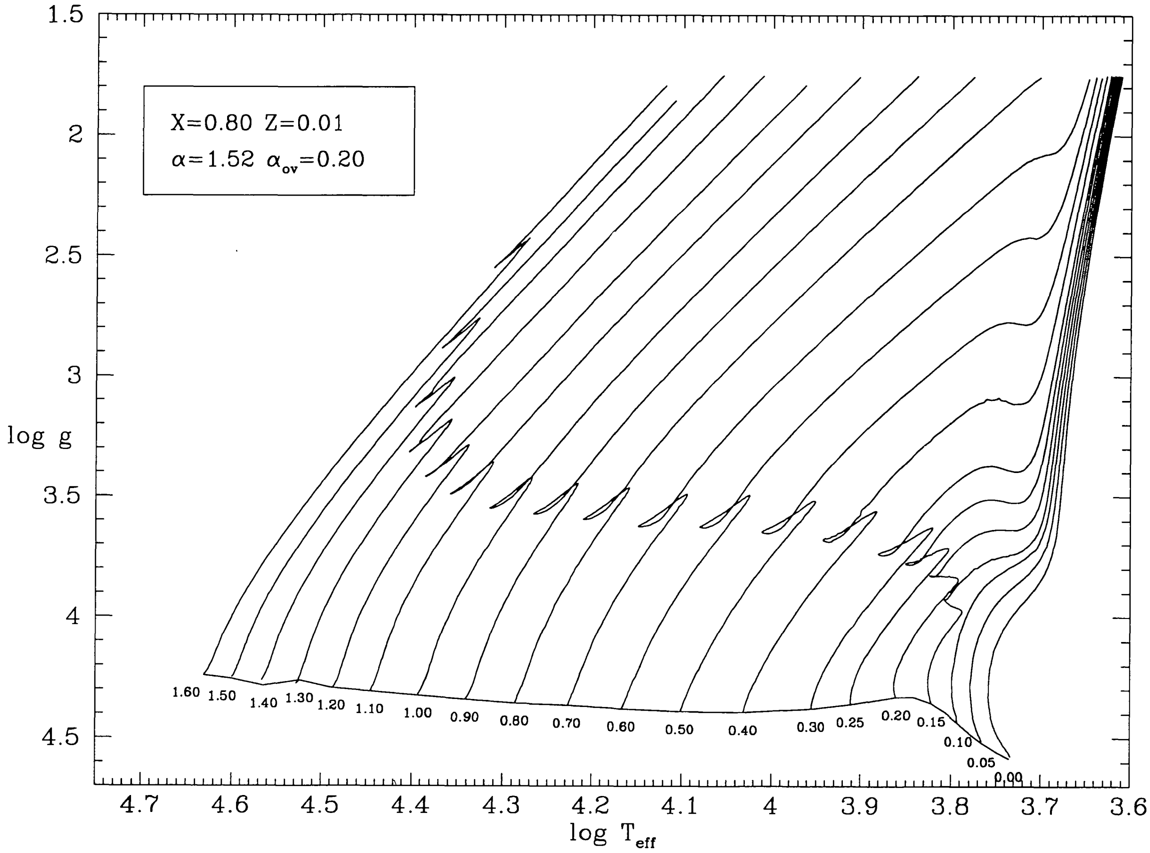

Fig. 6. Log g $-$log $T_{\rm eff}$ diagram for the grid X80. Numbers attached denote log M

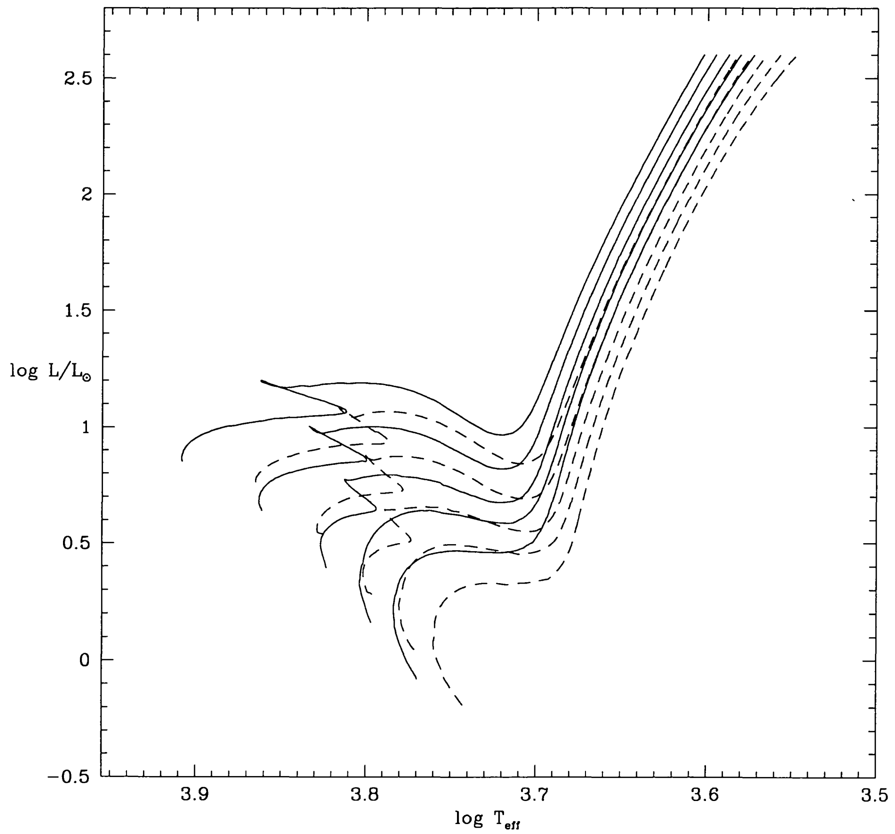

Fig. 7. Comparative HR diagram for Z=0.01, X=0.73 (full lines) and Z=0.02, X=0.70 (dashed lines). The select models are M=1.0, 1.12, 1.25, 1.41 and 1.58 $M_\odot$

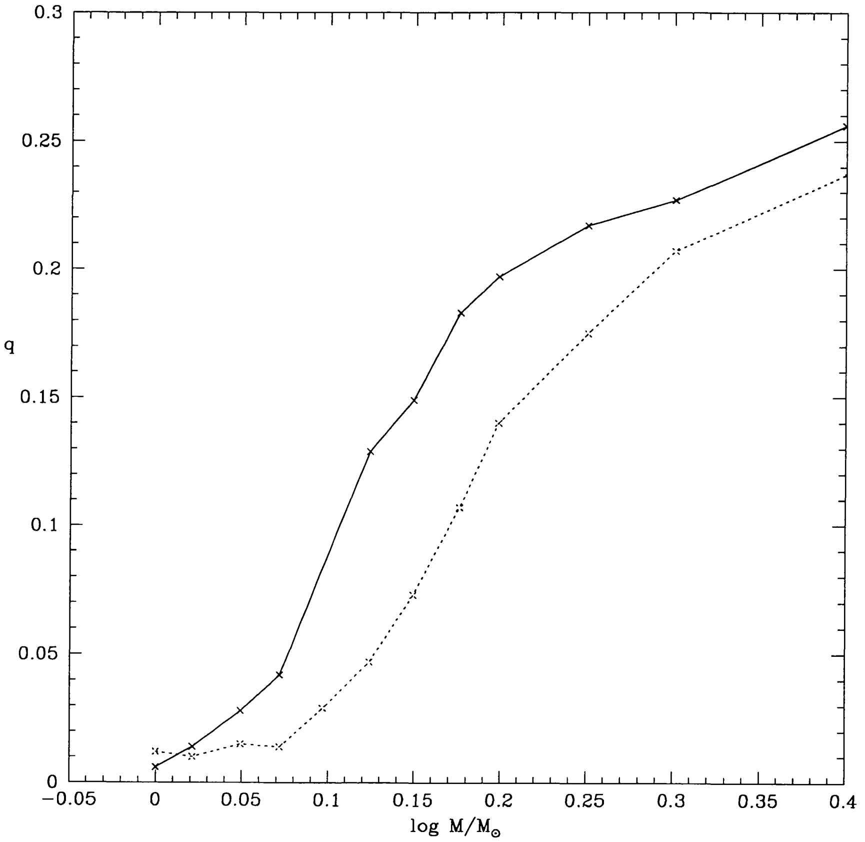

Fig. 8. Mass fraction of convective core as a function of the logarithm of the mass at the ZAMS. Full line represents the grid X63 while dotted denotes the grid X73. Note the increase of the mass with hydrogen content for which first develops a significant convective core

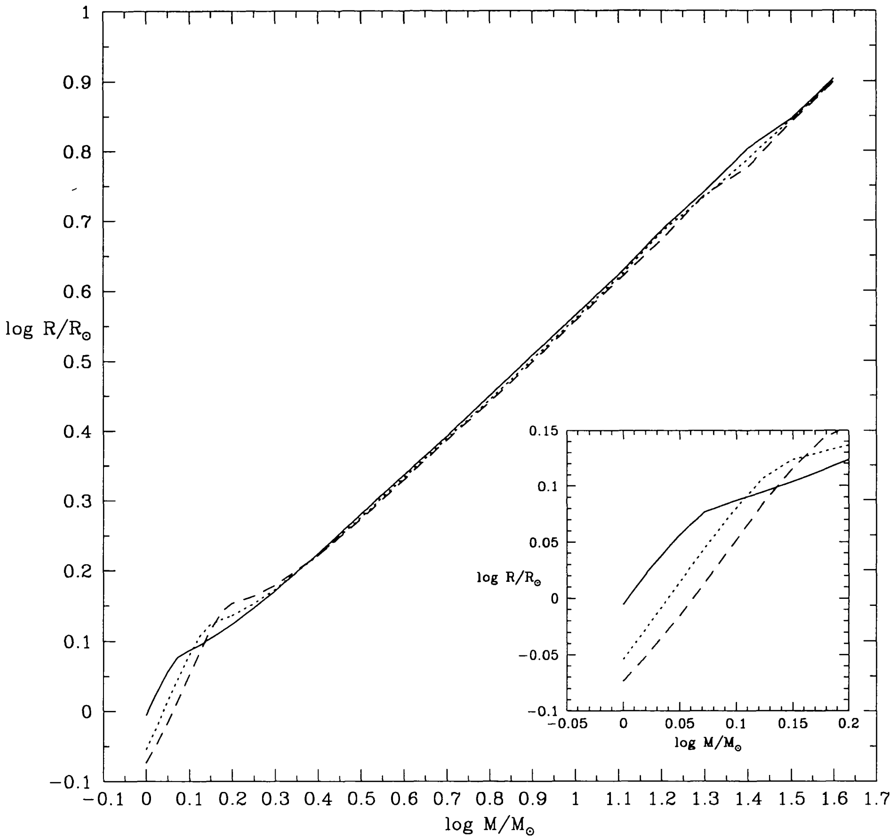

Fig. 9. Relation mass-radii for ZAMS models. The X63 set is represented by full line, dotted line denotes the set X73 and dashed line represents the set X80

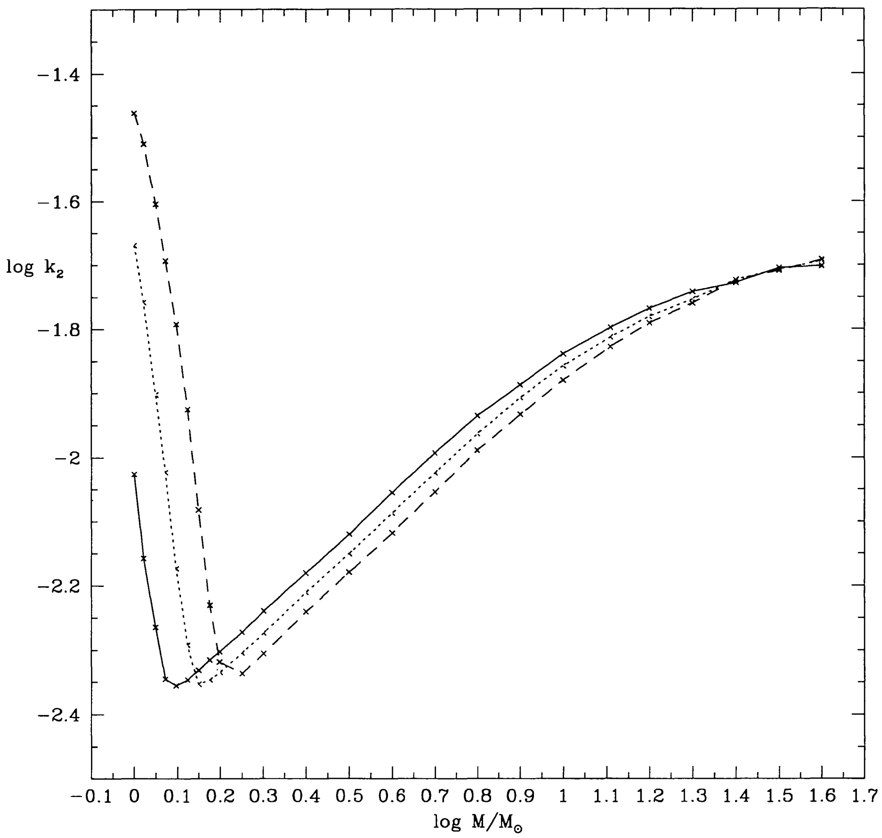

Fig. 10. The internal structure constants (log k_2) for ZAMS models. Same remarks as for Fig. 9